Defect-induced optical absorption in the visible range in ZnO nanowires

R. Michael Sheetz*
Center for Computational Sciences, University of Kentucky, Lexington, Kentucky 40506-0045, USA

Inna Ponomareva†
Department of Physics, University of South Florida, Tampa, Florida 33620-5700, USA

Ernst Richter‡
Daimler AG FGR/ESS, Wilhelm-Runge-Str. 11, 89081 Ulm, Germany

Antonis N. Andriotis§
Institute of Electronic Structure and Laser, FORTH, P.O. Box 1527, 71110 Heraklion, Crete, Greece

Madhu Menon‖
Department of Physics and Astronomy, University of Kentucky, Lexington, Kentucky 40506-0055, USA
and Center for Computational Sciences, University of Kentucky, Lexington, Kentucky 40506-0045, USA
(Received 15 July 2009; revised manuscript received 20 October 2009; published 17 November 2009)

The optical properties of ZnO nanowires containing defects are investigated using first-principles density-functional theory incorporating the LDA+U formalism. Calculations include defects in the form of substitutional N, Zn, and O vacancies as well as +1 charged O vacancy. Our calculations reveal that the presence of vacancies contribute strongly to optical absorption in the visible. Furthermore, the presence of +1 charged O vacancy is found to result in a blueshift of the absorption peaks, reducing the number of wavelengths that can be absorbed in the visible. These findings can be a useful tool for the design of new generation of materials with improved solar radiation absorption.

DOI: 10.1103/PhysRevB.80.195314 PACS number(s): 71.20.−b, 73.20.Hb, 75.30.Et, 75.30.Hx

I. INTRODUCTION

The photoluminescence (PL) emission of ZnO films displays emission in the ultraviolet (UV) (380 nm) and green (535 nm) spectral regions.[1] The UV emission is identified as originating at the band edge of ZnO and the green emission is attributed to defect related deep levels, especially the oxygen vacancies. The defects include oxygen vacancies, zinc vacancies, zinc interstitials, oxygen interstitials, and antisite defects (O_{Zn}), and all these point defects are controlled by growth conditions.[2] A recent experimental work seems to suggest the presence of ionized oxygen vacancy as responsible for this luminescence in the visible.[3]

In the nanowire form and at small diameters, quantum size effects are expected to influence all these applications. The quantum effects generally result in a substantial density of states (DOS) at the band edges thereby enhancing the radiative recombination due to carrier confinement. Furthermore, the recently reported stimulated emission and optical gain demonstrated in Si and CdSe nanoclusters[4,5] has generated expectation that similar gain may also be anticipated in ZnO nanowires.

Theoretical investigations of the optical properties of ZnO nanowires have been very few. The theoretical challenge stems from the highly correlated nature of the ZnO systems. The first-principles density-functional theory (DFT) based on the local density approximation (LDA) suffers from the well-known "gap problem." This is especially true for the highly correlated systems exhibiting strong effective Coulomb interactions between localized electrons, such as wide band-gap transition-metal oxides and perovskite-based ferroelectric materials. For these materials, LDA fails to give even reasonably accurate results for their band characteristics and especially electron energy gap values.[6–8] This is a serious drawback since the reliability of the optical calculations depends on the accurate determination of electronic band states.

An extension of the LDA method that has been found to correct this band-gap problem is the LDA+U method,[9,10] where the Hubbard parameter, U, is an on-site Coulomb repulsion parameter that incorporates part of the electron correlation absent in LDA. With an appropriate choice of U, as shown in the next section, the LDA+U method can reproduce the electronic energy bands accurately.

In this work we present results of theoretical calculations of the optical properties of pristine and doped ZnO nanowires of small diameter oriented in the (0001) direction. In the next section we describe the theoretical methods used in our calculations.

II. THEORETICAL METHODS

The theoretical calculations are performed using first-principles DFT using the LDA+U method implemented in the CASTEP program and employing norm-conserving pseudopotentials as implemented in the materials studio modeling and simulation software package.[11] We use this method to calculate the optical absorption coefficient since this is experimentally accessible.

While performing calculations of optical properties the common practice is to evaluate the complex dielectric con-

stant, $\varepsilon=\varepsilon_1+i\varepsilon_2$, and then express other properties in terms of it. The imaginary part of the dielectric constant is calculated using

$$\varepsilon_2(\mathbf{q}\to\mathbf{O}_{\hat{\mathbf{u}}},\hbar\omega)=\frac{2e^2\pi}{\Omega\varepsilon_0}\sum_{\mathbf{k},\mathbf{v},\mathbf{c}}|\langle\psi_{\mathbf{k}}^{c}|\hat{\mathbf{u}}\cdot\mathbf{r}|\psi_{\mathbf{k}}^{v}\rangle|^2\delta(E_{\mathbf{k}}^{c}-E_{\mathbf{k}}^{\mathbf{v}}-\hbar\omega), \tag{1}$$

where $\hat{\mathbf{u}}$ is the vector defining the polarization of the incident electric field. The sum in Eq. (1) involves k—integration over the Brillouin Zone by taking a symmetrized Monkhorst-Pack grid and smearing each energy level with a Gaussian spread function. After checking for convergence we use a $3\times2\times3$ Monkhorst and Pack mesh containing nine k points in the irreducible part of the Brillouin zone (IBZ).

The matrix elements that are required to describe the electronic transitions in Eq. (1), $\langle\psi_{\mathbf{k}}^{c}|\mathbf{r}|\psi_{\mathbf{k}}^{v}\rangle$, can be calculated in reciprocal space in a straightforward way when using local potentials. However, since nonlocal potentials are used in CASTEP, the corrected form of the matrix elements are:[12]

$$\langle\psi_{\mathbf{k}}^{c}|\mathbf{r}|\psi_{\mathbf{k}}^{v}\rangle=\frac{1}{im\omega}\langle\psi_{\mathbf{k}}^{c}|\mathbf{p}|\psi_{\mathbf{k}}^{v}\rangle+\frac{1}{\hbar\omega}\langle\psi_{\mathbf{k}}^{c}|[V_{nl}(\mathbf{r}),\mathbf{r}]|\psi_{\mathbf{k}}^{v}\rangle. \tag{2}$$

Since materials such as nanowires do not display full cubic symmetry, the optical properties will display some anisotropy. This can be included in the calculations by taking the polarization (defined by $\hat{\mathbf{u}}$ above) of the electromagnetic field into account. Therefore, when evaluating the dielectric constant there are three options for $\hat{\mathbf{u}}$: (i) define the direction of the electric-field vector for the light at normal incidence (polarized), (ii) represent the direction of propagation of incident light at normal incidence while the electric-field vector is taken as an average over the plane perpendicular to this direction (unpolarized) and, (iii) represent no specified direction, while the electric-field vectors are taken as a fully isotropic average (polycrystalline). In the present work we performed optical calculations using the polycrystalline polarization where the E field vector is an isotropic average over all directions. This allows us to obtain all of the peaks seen with the different incident light directions.

Reliable optical properties require an accurate determination of the electronic band gap. It should be noted that the LDA+U does not, in general, lead to the correction of the band gap. This is true, especially in the case of ZnO, if U is incorporated only for the d states. A correct gap can be obtained, however, if in addition to the U values for the d states, U values are included for the s or p states as well.[10] With this in view, we performed extensive tests to determine the appropriate U parameters for Zn(d), Zn(s), and O(p) that reproduced the correct energy for the Zn-3d DOS peak and the correct electronic band gap (3.4 eV) for bulk ZnO. The U values thus obtained are: $U_{d,\mathrm{Zn}}=10.5$ eV, $U_{s,\mathrm{Zn}}=0$, and $U_{p,\mathrm{O}}=7.0$ eV. The LDA+U method[13] was used to calculate the band structure, DOS, and optical properties of a ZnO nanowire (nw), ZnO nanowires containing either a single neutral oxygen (O) vacancy per supercell or a +1 charged O vacancy per supercell or a Zn-vacancy per supercell or a single N(O) atom substitution per supercell. All self-consistent calculations were carried out using a convergence criterion of 10^{-6} eV. The geometric structure of each nanowire was optimized using the generalized gradient approximation (GGA) and the Perdew-Burke-Ernzerhof (PBE) correlation functional prior to performing the LDA+U calculations. Spin-polarized LDA+U calculations were carried out using an energy cutoff of 600 eV.

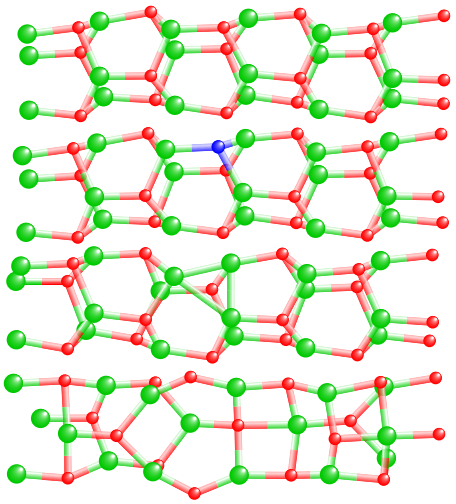

FIG. 1. (Color online) Side views of the fully relaxed structure of the defect-free ZnO nanowire (top) as well as ZnO nanowires containing defects. The Zn atoms are shown in green, while the O atom is shown in red. The defects include: substitutional N (second from top, N shown in blue), an O-vacancy (third from top) and a Zn-vacancy (bottom). The formation of vacancies results in significant structural changes on relaxation.

Each infinite nanowire was constructed from a supercell containing 36 atoms per cell by replication along the symmetry axis of the cell using periodic boundary conditions.

III. RESULTS

The relaxed structure of the defect-free ZnO nanowire as well as ZnO nanowires containing defects are shown in Fig. 1. The defects include: substitutional N (second from the top), an O vacancy (third from the top), and a Zn vacancy (bottom). The buckling is evident with the Zn atoms being pulled in more toward the nanowire axis. Substitution of an O atom with an N atom, however, results in minimal structural change on relaxation. We have performed detailed analysis of electronic band structure and DOS for all these structures as well as the projected density of states (PDOS) for individual atoms. The band gap for the defect-free ZnO nanowire, 3.72 eV, is larger than that for bulk ZnO obtained with the same U parametrization. The PDOS for this nanowire shows the Zn d state to be situated deeper in the valence band and, therefore, less relevant, while the O p state to dominate the bands near the Fermi energy. Interestingly, the conduction bands show a mixture of both Zn and O orbitals. For the case of substitutional N (Fig. 1, second from top), the electronic band structure and DOS are almost identical to the defect-free ZnO nanowire. Removal of an O atom to create a vacancy, however, results in significant structural changes on relaxation. The three Zn neighbors to the removed O now

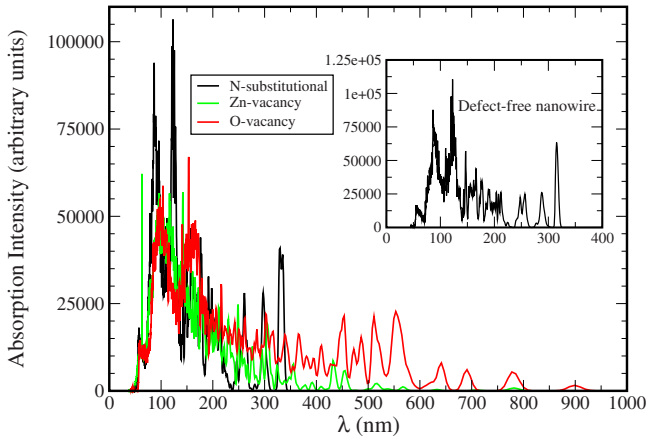

FIG. 2. (Color online) Calculated optical absorption spectrum of the ZnO nanowires containing defects in the form of substitutional N, O-vacancy and Zn-vacancy shown in Fig. 1 along with that of the defect-free nanowire (inset) for comparison. The spectrum shows several absorption peaks within the visible range in the presence of vacancies.

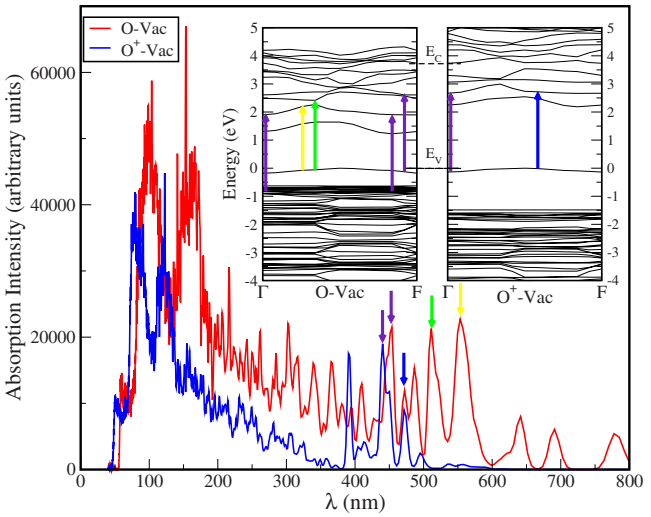

FIG. 3. (Color online) The optical absorption of +1 charged O-vacancy in ZnO nanowire along with that of the neutral vacancy. The spectrum for the charged vacancy, while retaining absorption peaks in the visible range, shows a significant blue shift of the intensity peaks. The transitions responsible for the different colors in the visible range are indicated in the band structure diagrams in the inset. The valence band maximum and the conduction band minimum of the defect-free ZnO nanowire are indicated by E_V and E_C, respectively.

come closer to form bonds in the form of a triangle (Fig. 1, third from top). Creation of a Zn vacancy causes maximum structural distortion on relaxation with the entire supercell being affected (Fig. 1, bottom). The three O atoms nearest to the vacancy move farther away from each other causing a partial "opening" up of the nanowire near the vacancy site. This is in contrast to the case of O vacancy where the surrounding Zn atoms move toward each other and form bonds.

The atomic displacements resulting from structural relaxation on vacancy creation have significant effects on the electronic structures of the nanowires. In the case of O vacancy, analysis of the partial DOS shows the valence states near the Fermi level to be mainly a hybrid with mixed O $2p$ (second nearest neighbors to the O vacancy) and Zn $3d$, although dominated by the O $2p$ states. The energy levels in the gap, however, draw their contributions almost exclusively from the O $2p$ states. The Zn $3d$ contribution is deep down in the valence bands. In the case of the Zn vacancy, the valence states near the Fermi level are entirely derived from O $2p$ states, while the Zn $3d$ states move deeper into the valence bands. Energy levels appear deep in the gap as in the O vacancy case with the gap region dominated by O $2p$ states. The presence of deep level O $2p$ states caused by the formation of O and Zn vacancies now allow for electronic transitions to these levels from the valence states. In particular, the possibility of allowable transitions within the visible range becomes feasible.

The calculated optical absorption spectrum for the nanowires in Fig. 1 is shown in Fig. 2. We obtain the spectra by calculating the imaginary part of the complex dielectric function using Eq. (1) within the spin-polarized LDA+U method as implemented in CASTEP. The allowed transitions are determined by the nonzero matrix elements of the position operator. A total of 100 empty bands were included in the calculation with an energy cutoff of 600 eV for the optical properties for each of the ZnO nanowires. The optical calculations are performed using the "polycrystalline" polarization where the E field vector is an isotropic average over all directions. In the calculations of the spectra we use a rather small smearing of 0.02 eV in order to better distinguish the absorption peaks. As can be seen, the absorption peak for the defect-free nanowire (see inset to Fig. 2) is well below the threshold for the visible (400 nm). This is because of the relatively large band-gap value of 3.72 eV for the defect-free nanowire. The near band-edge absorption corresponding to the largest wavelength is, therefore, just above 300 nm.

While the absorption spectra for the nanowire with substitutional N shows no peaks in the visible, those for Zn and O vacancies show several relatively broader peaks in the visible. The peaks for the O vacancies are far more intense than that for the Zn-vacancy. In particular, there are three peaks showing maximum intensities at wavelengths 453, 511, and 553 nm corresponding to indigo, green, and yellow colors, respectively.

Although the absorption spectra cannot be compared directly to the photoluminescence spectra in total, nevertheless, it is interesting to discuss the theoretical absorption spectra in light of the reported experimental photoluminescence spectra of various ZnO nanostructures. While the absorption results from excitation of the electron by the incoming light, photoluminescence results from subsequent transition to lower energy levels which may also include intermediate energy levels allowed by the transition rules in addition to the original level. The ZnO nanostructures synthesized have been reported to exhibit three emissions in the visible range (green, yellow, and red) which were assigned to three different types of defects based on depth resolved cathodoluminescence and PL measurements.[14] This is in addition to the UV emission corresponding to the near band-edge emission common to these materials. In view of these our finding of ab-

sorption peaks in the visible range is relevant since one of the defects responsible for photoluminescence has been identified as the O vacancy by experiments.[15–17]

We have also considered the optical absorption of +1 charged O vacancy in ZnO nanowire. The absorption spectra are shown in Fig. 3 along with that of the neutral vacancy. As can be seen, while retaining absorption peaks in the visible range, there is a significant blueshift of the intensity peaks. The two main peaks at wavelengths 440 and 450 nm correspond to indigo and blue colors, respectively.

Since the electronic transitions responsible for absorption are connected to the electronic structure of the system, it is instructive to examine the band structure in the case of the O vacancy. In the left inset to Fig. 3 we show the electronic band structure for the ZnO nanowire containing neutral O vacancy, while the band structure for the +1 charged O vacancy is on the right. The valence-band maximum and the conduction band minimum of the defect-free ZnO nanowire are indicated by E_V and E_C, respectively. As can be seen, there are several vacancy induced states deep in the band gap that permit electronic transitions as a result of optical absorption in the visible. The allowed transitions corresponding to the absorption peaks are indicated by the arrows. In the case of the +1 charged O vacancy, the structural relaxation results in further lowering of the valence band states with the exception of the highest occupied lone band. There is a corresponding raising of the unoccupied deeper band-gap states. This in turn causes an increase in the absorption energies resulting in the blue shift of the absorption peaks, reducing the number of wavelengths that can be absorbed in the visible.

In summary, our detailed investigations of optical properties reveal that the presence of defects in ZnO nanowires in the form of vacancies contribute strongly to optical absorption in the visible. The presence of charge seems to weaken this absorption. The present findings can be a useful tool for the design of new generation of materials with improved solar radiation absorption. The geometry of nanowires offer naturally large surface to bulk ratio. Combining this feature with the creation of O vacancies can, therefore, result in maximizing solar energy absorption for useful applications.

ACKNOWLEDGMENTS

The present work is supported through grants by DOE (Grants No. DE-FG02-00ER45817 and No. DE-FG02-07ER46375).

*rmshee0@email.uky.edu
†iponomar@cas.usf.edu
‡ernst.richter@daimler.com
§andriot@iesl.forth.gr
‖madhu.menon@uky.edu

[1] X. L. Wu, G. G. Siu, C. L. Fu, and H. C. Ong, Appl. Phys. Lett. **78**, 2285 (2001).
[2] T. Koida, S. F. Chichibu, A. Uedono, A. Tsukazaki, M. Kawasaki, and T. Sota, Appl. Phys. Lett. **82**, 532 (2003).
[3] Y. Hu and H. J. Chen, J. Appl. Phys. **101**, 124902 (2007).
[4] V. I. Klimov, A. A. Mikhailovsky, S. Xu, A. Malko, J. A. Hollingsworth, C. A. Leatherdale, H. J. Eisler, and M. G. Bawendi, Science **290**, 314 (2000).
[5] L. Pavesi, L. D. Negro, C. Mazzoleni, G. Granzo, and F. Priolo, Nature (London) **408**, 440 (2000).
[6] J. P. Perdew and M. Levy, Phys. Rev. Lett. **51**, 1884 (1983).
[7] H. Odaka, S. Iwata, N. Taga, S. Ohnishi, Y. Kaneta, and Y. Shigesato, Jpn. J. Appl. Phys. **36**, 5551 (1997).
[8] C. Kilic and A. Zunger, Phys. Rev. Lett. **88**, 095501 (2002).
[9] A. Walsh, J. L. F. DaSilva, and S.-H. Wei, Phys. Rev. Lett. **100**, 256401 (2008).
[10] N. N. Lathiotakis, A. N. Andriotis, and M. Menon, Phys. Rev. B **78**, 193311 (2008).
[11] M. D. Segall, P. J. D. Lindan, M. J. Probert, C. J. Pickard, P. J. Hasnip, S. J. Clark, and M. C. Payne, J. Phys.: Condens. Matter **14**, 2717 (2002).
[12] A. J. Read and R. J. Needs, Phys. Rev. B **44**, 13071 (1991).
[13] I. Nekrasov, M. Korotin, and V. Anisimov, arXiv:cond-mat/0009107 (unpublished).
[14] H. C. Ong and G. T. Du, J. Cryst. Growth **265**, 471 (2004).
[15] C. Chandrinou, N. Boukos, C. Stogios, and A. Travlos, Microelectron. J. **40**, 296 (2009).
[16] A. B. Djurišić, Y. H. Leung, K. H. Tam, L. Ding, W. K. Ge, H. Y. Chen, and S. Gwo, Appl. Phys. Lett. **88**, 103107 (2006).
[17] H. Q. Wang, G. Z. Wang, L. C. Jia, C. J. Tang, and G. H. Li, J. Phys. D **40**, 6549 (2007).